Available online at www.sciencedirect.com
ScienceDirect
Polymer 48 (2007) 1756–1769
polymer
www.elsevier.com/locate/polymer

Isothermal crystallization behavior of isotactic polypropylene blended with small loading of polyhedral oligomeric silsesquioxane

Jean-Hong Chen*, Bo-Xian Yao, Wen-Bin Su, Yao-Bin Yang

Department of Polymer Materials, Kun Shan University, Yung-Kang City, Tainan Hsien 710032, Taiwan, ROC

Received 4 July 2006; received in revised form 4 December 2006; accepted 8 January 2007
Available online 12 January 2007

Abstract

The isothermal crystallization kinetics and morphology development of isotactic polypropylene (iPP) blended with small loading of nanostructure of polyhedral oligomeric silsesquioxane (POSS) were studied with differential scanning calorimetry (DSC), polarized optical microscopy (POM), and wide-angle X-ray diffraction (WAXD). The crystallization behaviors of iPP/POSS composites presented an unusual crystallization behavior during isothermal and nonisothermal crystallization conditions. The exothermic morphologies of isothermal and nonisothermal crystallization of iPP/POSS composites changed remarkably with increasing POSS. Moreover, the developments of spherulitic morphology for iPP/POSS composites showed that the major dispersed POSS molecules became nanocrystals first and then aggregated together forming thread- or network-like morphologies, respectively, depending on POSS content, which was observed. It implies that these major POSS nanocrystals' morphologies appeared as an effective nucleating agent and promoted the nucleation rate of iPP, whereas the minor dispersed POSS molecules that had slight miscibility between iPP retarded the nucleation and growth rates of iPP in the remaining bulk region. Therefore, the isothermal crystallization showed a single exothermic peak at pure iPP and POSS-1.0, whereas at POSS-2.0 and POSS-3.0, displayed the multi-exothermic peaks during isothermal crystallization. These faces indicated that POSS molecules were both influence on the transport of iPP chain in the melted state and on the free-energy of formation the critical nuclei of iPP assisted by the POSS structures were observed. Therefore, we postulated that the crystallization mechanisms of multi-exothermic peaks in isothermal crystallization may proceed to combine the "*nucleating agent inducing nucleation of iPP event assisted by the POSS domains*" that the nucleation of iPP does occur preferentially on the surfaces of the POSS "threads" or "networks" structures, and "*nucleation and growth of iPP in the remaining bulk melted iPP region retarded by dispersed POSS molecules*". Therefore, effects of POSS content on the isothermal and nonisothermal crystallization behaviors of iPP/POSS composites due to the POSS molecules partially miscible with iPP, at very small loading of POSS molecules, promoted or retarded the rates of nucleation and growth of iPP depending on the POSS content and crystallization temperature were discussed.

Keywords: Isothermal crystallization kinetics; iPP/POSS composites; Spherulitic morphology

1. Introduction

It is well known that isotactic polypropylene (iPP) exhibits several crystalline forms at different processing conditions. All these crystal forms are affected not only by molecular mass and molecular mass distribution of iPP but also by different blending compounds and preparation conditions, i.e., isothermal temperature and nucleating agents used. The use of nucleating agents in polymers is extensive and becomes an important process because the control of the crystallization behavior allows to modify the microstructure that retards or enhances the physical properties of polymers, such as thermal, mechanical and so on. However, the physical properties of polymers are essentially controlled by the adjustment of type and dispersion of the nucleating agent blended with polymer matrix. Therefore, the blending with nucleating agents in polymer attracts much interests because the relationship between the structure of nucleating agents and the physical properties of polymer matrix is very complicated [1–8].

* Corresponding author. Tel.: +886 6 205 5138; fax: +886 6 205 0493.
E-mail address: kelvench@mail.ksu.edu.tw (J.-H. Chen).

0032-3861/$ - see front matter © 2007 Elsevier Ltd. All rights reserved.
doi:10.1016/j.polymer.2007.01.010

Recently, the cage-shaped polyhedral oligomeric silsesquioxane (POSS) molecules are new classes of nanoparticles in the polymer science and attract much research groups' interest. The POSS molecules can be dispersed in many polymers by the adjustment of the functionalized substituents on the POSS cage through synthetic routes such as copolymerization and chemical grafting or by physical mixing. Copolymerization is an efficient approach to POSS nanocomposites due to the formation of chemical bonds or chemically linked between POSS molecules and polymer materials and enhanced mechanical performance, higher glass transition temperature and higher thermal decomposition temperature [9–18]. Compared to the chemically modified POSS nanocomposites, relatively few researchers have studied physically blended POSS nanocomposites due possibly to the unfavorable miscibility of POSS with polymer [4–8]. More recently, Hsiao et al. first studied the crystallization behavior at quiescent and shear states of iPP/POSS composites. The octamethyl-POSS was added by melt blending with iPP at quite large concentrations and the crystallization behavior was studied by means of DSC and in situ SAXS measurements [4]. They reported that the POSS, acting as a nucleating agent, was found to influence the quiescent melt crystallization enhancing or retarding the crystallization process, depending on POSS concentration at very large loading of POSS. Then, they have also investigated the physical gelation in ethylene–propylene (EP) copolymer melts induced by POSS molecules. EP/POSS composites were prepared by melt mixing in a twinscrew microcompounder with EP copolymers characterized by different ethylene contents and varying the POSS loadings from 10 to 30 wt% [5]. The results of WAXD indicated that no molecular dispersion of POSS cages could be achieved as POSS X-ray pattern was maintained in the composites. Small-amplitude oscillatory shear experiments showed that the EP/POSS composites exhibited a solid-like rheological behavior above melting compared with the liquid-like behavior in the neat resin. Moreover, the addition of 10 wt% of POSS was found to increase considerably the Young's modulus and the T_g value as compared to neat EP. More recently, the influence of functionalization of POSS cages on the iPP/POSS has been reported by Fina et al. [6]. They indicated that a good dispersion of POSS was obtained particularly at low loadings of POSS with longer organic chains. On the other hand, the nonisothermal crystallization of HDPE/POSS nanocomposites has been studied by Joshi and Butola [7]. They reported that the value of Avrami exponent n for HDPE/POSS (90:10) nanocomposite ranged from 2.5 to 2.9 and its decrease with increasing cooling rate is caused by spherulitic crystal growth with heterogeneous nucleation, while simultaneous occurrence of spherulitic and lamellar crystal growths with heterogeneous nucleation accounted for lower values of n at higher cooling rates. However, they indicated that presence of POSS molecules did not cause significant change in the activation energy for the transport of polymer segments to the growing crystal surface. POSS molecules exhibit nucleation activity only at 10 wt% loading in HDPE and are not effective nuclei at lower loadings.

Therefore, the crystallization behavior and morphology development of isothermally crystallized iPP/POSS nanocomposites, at very small loading of POSS, as a function of POSS content have been reported recently [8]. We indicated higher T_g and lower E' of iPP/POSS nanocomposites than that of the pure iPP, moreover, the thermal properties, such as T_m^m and T_m^{rm}, of iPP/POSS nanocomposites slightly decreased, while ΔH_f^m, ΔH_f^{rm} and crystallization ability of iPP/POSS nanocomposites increased with POSS. The morphologies indicated that the POSS molecules became about 35 nm nanocrystals and aggregated to form thread-like and network structure morphologies, respectively, in molten state of iPP at very small loading of POSS. Therefore, influences of the POSS molecules on the isothermal crystallization behavior and crystallization kinetics of the iPP/POSS composites, especially at very small loading of POSS molecules, are still a question unresolved.

In the present article, the isothermal and nonisothermal crystallization behaviors of physically blended iPP/POSS composites were studied with differential scanning calorimetry (DSC), wide-angle X-ray diffraction (WAXD), and polarized optical microscopic (POM) techniques. The aim of this article is to compare the isothermal and nonisothermal crystallization behaviors of iPP/POSS composites at very small loadings of POSS. The Avrami equation is used for the analysis of the isothermal crystallization kinetics of pure iPP and iPP/POSS composites. DSC thermograms provided the necessary crystallization kinetics data and POM observation is also made to measure the relationship between the POSS contents and the spherulitic morphology of iPP/POSS composites.

2. Experimental

2.1. Materials and blend preparation

The isotactic polypropylene with a weight-average molecular weight of $M_w = 3.4 \times 10^5$ g mol^{-1} and POSS nanoreinforced polypropylene containing 10 wt% octamethyl-POSS were purchased from Aldrich Chemical. In this study, the chosen POSS molecules have an empirical formula $(RSiO_{1.5})_8$, where R group was substituted with methyl. Melt-blended specimens of these materials with various compositions were prepared by a twinscrew apparatus (MP2015 APV Chemical Machinery Co. Ltd, U.S.A.) at 230 °C. The mixing ratios of POSS molecules in iPP matrixes were 0, 0.5, 1.0, 2.0, and 3.0 wt%/wt% and defined these composites as pure iPP, POSS-0.5, POSS-1.0, POSS-2.0, and POSS-3.0. The thermal properties of iPP/POSS composites used in this study are compiled in Table 1.

The compression-molded films were prepared by melt pressing of iPP/POSS composites for a molding of 120 × 120 × 1 mm^3. All samples were molten at 230 °C and held at this temperature for 10 min to allow complete melting, and then these iPP blends' mold was taken out and immediately submerged in a temperature controlled compression molding machine at different crystallization temperatures, T_c, with the temperature intervals of 3 °C from 115 to

Table 1
Thermal properties of iPP/POSS composites studied in this work

Materials	T_c[a] (°C)	ΔH_c[a] (J/g)	T_m[b] (°C)	ΔH_f[b] (J/g)	$\chi_{c,iPP}$[c] (%)	T_m^o (°C)
Pure iPP	104.07	−86.39	168.34	87.74	41.94	187.8
POSS-0.5	112.01	−79.87	167.04	81.93	39.16	187.2
POSS-1	112.22	−82.52	166.67	89.84	42.94	185.9
POSS-2	115.05	−83.64	166.67	89.75	42.90	186.6
POSS-3	112.67	−84.64	166.34	91.43	43.71	186.6

[a] Calculated from crystallization exothermic of DSC cooling trace after melted.
[b] Calculated from melting endotherm of DSC heating trace after isothermal crystallization at 130 °C.
[c] The crystallinity of iPP calculated from the measured enthalpies of fusion, ΔH_f, of iPP for iPP/POSS composites after isothermal crystallization at 130 °C ($\Delta H_{f\,iPP}^o = 209.2$ J/g).

135 °C, under a pressure of 50 kg cm^{-2}, where it was still placed between the two steel platens and held for 120 min for necessary isothermal crystallization.

2.2. Measurements

2.2.1. Thermal properties of iPP/POSS composites

The thermal properties of iPP/POSS composites were determined with a Perkin–Elmer PYRIS Diamond DSC with an intra-cooler at lowermost temperature of about −65 °C. About 5 mg of samples were cut from the isothermally crystallized iPP/POSS composites, put into the sample pan, heated to 230 °C in the furnace in a nitrogen atmosphere at a rate of 10 °C min^{-1} and the melting thermogram was measured. The temperature and area of the endothermic curve were taken as the melting temperature, T_m, and the heat of fusion, ΔH_f, respectively. When temperature reaches 230 °C, samples were maintained for 10 min in order to eliminate any previous thermal history, and followed by a cooling rate of 10 °C min^{-1} the crystallization thermogram was measured. The temperature and area of the exothermic curve were taken as the crystallization temperature, T_c, and the latent heat of crystallization, ΔH_c, respectively. These thermal properties results are also shown in Table 1.

2.2.2. Dynamic crystallization kinetics of iPP/POSS composites

Dynamic crystallization kinetics of iPP/POSS nanocomposites were also carried out with PYRIS Diamond DSC. About 7 mg of isothermally crystallized samples were sealed in aluminum pans and melted in the furnace in a nitrogen atmosphere at 230 °C for 10 min in order to eliminate any previous thermal history and then they were rapidly quenched to desired crystallization temperature, T_c at a cooling rate of 400 °C min^{-1} and maintained at this temperature during the time necessary for isothermal crystallization process.

2.2.3. WAXD

Wide-angle X-ray diffraction intensity curve of isothermally crystallized iPP/POSS nanocomposites was measured with a graphite-monochromatized Cu Kα radiation generated at 40 kV and 180 mA in a Rigaku D/Max 2500VL/pc diffractometer. WAXD intensities were recorded from $2\theta = 5°$ to 35° with a continuous scanning speed of $2\theta = 1°$ min^{-1} with data collection at each 0.05° of 2θ.

2.2.4. Polarized optical microscopy

Spherulitic morphologies of iPP/POSS nanocomposites were investigated using a polarized optical microscope of Zeiss Axioskop-40 with a Linkam-TH600 hot stage. The samples, inserted between two microscope cover glasses, were melted at 230 °C and squeezed to obtain thin films. The thin film samples were inserted in hot stage. Each sample was heated from 30 to 230 °C at a rate of 20 °C min^{-1}, kept at this temperature for 10 min to allow complete melting, followed by cooling to isothermal crystallization temperature at a rate of 90 °C min^{-1} and maintained at this temperature during the time necessary for isothermal crystallization. The temperature of hot stage can be kept constant within 0.1 °C and dry nitrogen gas was purged through the hot stage during measurement.

3. Results and discussion

3.1. Nonisothermal crystallization behavior of iPP/POSS composites

Polymer crystallization is usually preceded by homogeneous nucleation, heterogeneous nucleation, or self-nucleation and then by growth of the crystal with crystallization time. However, a crystallizable polymer, nucleation may caused by homogeneous or by heterogeneous (impurities, nucleating agent, or others), which can controls the microstructure and physical properties of polymer. Therefore, overall crystallization behavior of polymers can be analyzed by the observation of the rates of nucleation and growth or the overall rate of crystallization of polymers which can forecast relationship between the microstructures and preparation conditions of the polymers. Thus, Fig. 1 shows the nonisothermal crystallization behavior of iPP/POSS composites as a function of POSS content at cooling trace of DSC. For pure iPP, it shows a higher-temperature shoulder in front of the main exothermic peak. In contrast, all iPP/POSS composites only show a single exothermic peak and increase in the crystallization temperature, at very small loading of POSS, with increasing POSS was observed. Both the latent heat of crystallization, ΔH_c, and crystallization temperature, T_c, of iPP/POSS composites increase evidently with increasing POSS. Moreover, the time needed to reach the maximum of exothermic peak during nonisothermal crystallization, t_{em}^{uni}, decreases remarkably with increasing POSS at cooling trace. However, the exothermic peak corresponds with both rates of nucleation and growth of iPP/POSS composites during nonisothermal crystallization. The higher-temperature shoulder in front of the main exothermic peak of pure iPP indicates a homogeneous nucleation process, whereas all iPP/POSS composites show a heterogeneous nucleation process implying that the POSS molecules essentially act as an effective nucleating agent for iPP matrix and promote

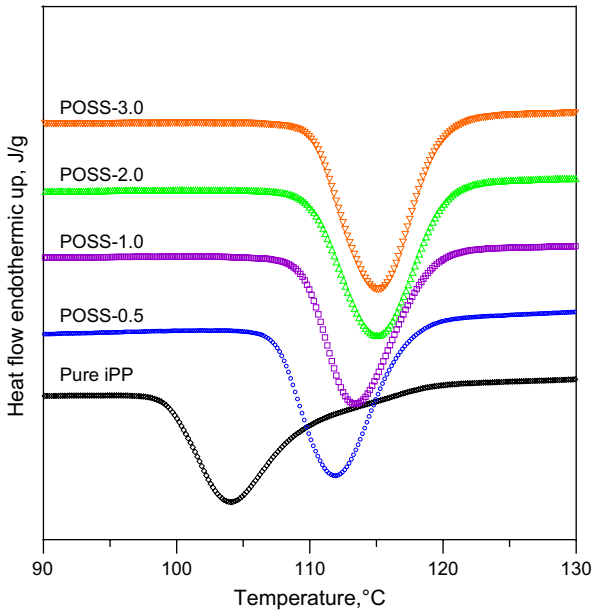

Fig. 1. Influence of POSS contents on the nonisothermal crystallization exotherm of iPP/POSS composites at cooling trace.

the crystallization rate of iPP during nonisothermal crystallization. Therefore, as POSS molecule was increased, the crystallization behavior of iPP/POSS composites changes remarkably and increase in T_c with increasing POSS was observed.

3.2. Isothermal crystallization kinetics of iPP/POSS composites

According to the above results, the effects of POSS content on the isothermal crystallization kinetics of iPP/POSS composites are very important and still a question unresolved. Recently, Hsiao et al. reported that the POSS molecules act as a nucleating agent which enhances or retards the crystallization process, depending on quite large loading of POSS concentration [4]. On the other hand, the value of Avrami exponent n for HDPE/POSS (90/10) nanocomposite ranged from 2.5 to 2.9 and its decrease with increasing cooling rate was caused by spherulitic crystal growth with heterogeneous nucleation, while simultaneous occurrence of spherulitic and lamellar crystal growths with heterogeneous nucleation accounts for lower values of n at higher cooling rates has been reported by Joshi and Butola [7]. However, they indicated that the POSS molecules exhibit nucleation activity only at 10 wt% loading in HDPE and are not effective nuclei at lower loadings. The effects of small loading of POSS content on the crystallization behavior and morphology development of iPP/POSS composites have also been reported recently. We concluded that the interaction between POSS molecules dominated the crystallization/nucleation behavior and aggregated POSS nanocrystals to form thread-like and network structure morphologies in molten state of iPP/POSS nanocomposites. However, the interaction between POSS molecules and iPP matrix should be increased with increasing chain length of functionalized substituents on the POSS cage due to increasing miscibility between the POSS molecule and iPP, which has been reported recently [8]. The effects of the POSS content on the isothermal crystallization behavior of iPP/POSS composites at very small loading of POSS are very interesting and still a question unresolved. Therefore, in this work, the effects of POSS content on the isothermal crystallization behavior of iPP/POSS composites even at very low POSS content were investigated.

Generally, analysis of the isothermal crystallization kinetics of polymers and polymer composites was performed using the classical Avrami equation [19,20] as given in Eq. (1)

$$1 - X(t) = \exp(-kt^n) \tag{1}$$

where $X(t)$ is the development of crystallinity, X_c, at time t, the k and n values denote the crystallization rate constant and the Avrami exponent, respectively. Both k and n depend on the nucleation and growth mechanisms of spherulites. The fraction of $X(t)$ is obtained from the area of the exothermic peak of isothermal crystallization analysis in DSC at a crystallization time t divided by the total area under the exothermic peak as shown in Eq. (2)

$$X(t) = \frac{X_c(t)}{X_c(t=\infty)} = \frac{\int_0^t (dH/dt)dt}{\int_0^\infty (dH/dt)dt} = 1 - \exp(-kt^n) \tag{2}$$

where the numerator is the heat generated at time t and the denominator is the total heat generated up to the complete crystallization. It should be noted that t is the time spent during the course of crystallization measured from the onset of crystallization. In order to deal conveniently with the operation, Eq. (1) is usually rewritten as double logarithmic form as follows:

$$\log\{-\ln[1 - X(t)]\} = \log k + n \log t \tag{3}$$

According to Eq. (3), when plotting $\log\{-\ln[1 - X(t)]\}$ against $\log t$, the n and k values could be directly obtained as the slope and the antilogarithmic value of the y-intercept, respectively. Based on Eq. (1), if the time the polymer spends from the beginning of the crystallization process to the time at which a certain amount of relative crystallinity has been developed is known, the half-time of crystallization, $t_{1/2}$, can also be directly calculated as follows:

$$t_{1/2} = \left(\frac{\ln 2}{k}\right)^{1/n} \tag{4}$$

In order to analyze the effect of POSS content and T_c on the isothermal crystallization kinetics of iPP/POSS composites with Avrami equation, the isothermal crystallization behaviors for pure iPP, POSS-1.0, POSS-2.0 and POSS-3.0, respectively, at various crystallization temperatures are presented in Fig. 2. As result from Fig. 2 indicates that the time to reach the maximum of exothermic peak of isothermal crystallization order,

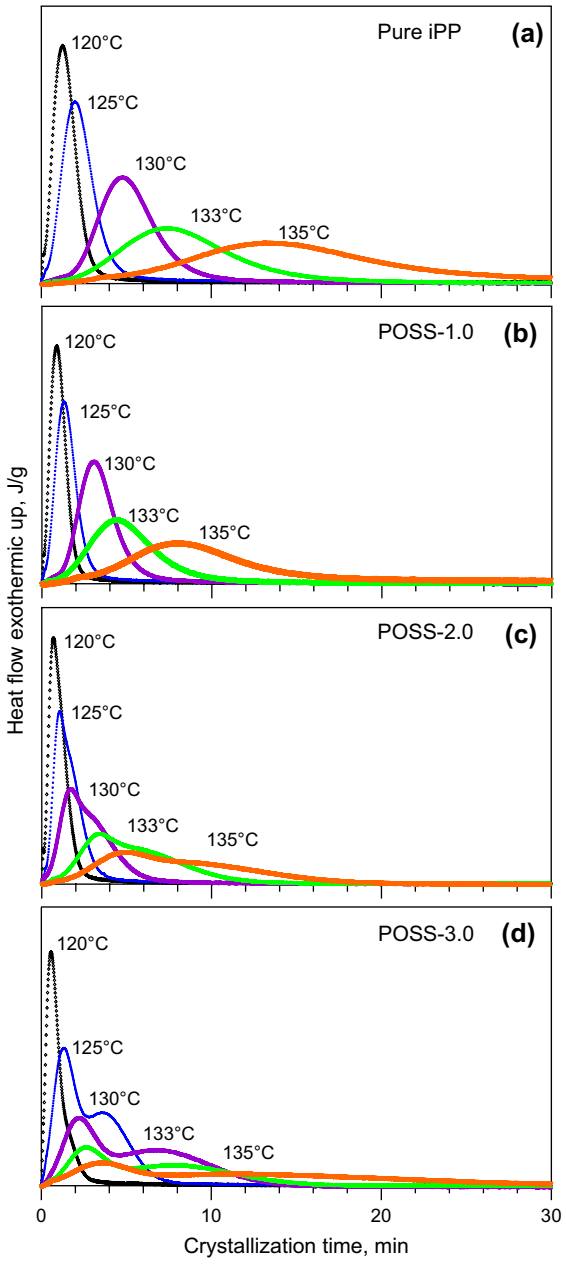

Fig. 2. Effect of POSS contents and crystallization temperature on the isothermal crystallization kinetics of iPP/POSS composites: (a) pure iPP, (b) POSS-1.0, (c) POSS-2.0, and (d) POSS-3.0.

t_{em}^{iso}, of iPP/POSS composites decreases as the supercooling temperature, ΔT, and POSS content were increased. At the same isothermal temperature, the t_{em}^{iso} of almost all iPP/POSS composites is rapider than that of pure iPP. It is interesting to note that the isothermal crystallization morphology of pure iPP and POSS-1.0 shows a single exothermic peak at all temperatures, comparatively that of POSS-2.0 and POSS-3.0 show the multi-exothermic peaks' behaviors at higher T_c. It indicates that, on comparing pure iPP with iPP-1.0, the crystallization mechanism of pure iPP proceeds mainly via homogeneous nucleation mechanism, while that of POSS-1.0 may proceed by heterogeneous nucleation mechanism, respectively, as the results of POM shown in Fig. 8(a–b) and (c–d). On the other hand, the isothermal crystallization mechanisms for both POSS-2.0 and POSS-3.0 precede the multi-crystallization mechanisms during isothermal crystallization. This result indicates that the crystallization mechanisms of POSS-2.0 and POSS-3.0 may combine the heterogeneous and homogeneous nucleations together and then follow the crystal growth during isothermal crystallization. The homogeneous nucleation starts spontaneously by polymer chain aggregation below the melting point, therefore it requires a longer crystallization time, whereas heterogeneous nuclei form simultaneously as soon as the sample reaches the crystallization temperature, which is also clearly shown in Fig. 8. At the same temperature, with increasing POSS the first peak of multi-crystallization mechanisms decreases, whereas the second peak of multi-crystallization mechanisms increases. In this work, the first peak of multi-crystallization mechanisms implies that the crystallization of iPP with the nucleation event is assisted by the POSS domains because the POSS essentially act as a nucleating agent; therefore, the nucleation of iPP does occur preferentially on the surfaces of the thread or network structures of POSS. Whereas, the second peak of multi-crystallization mechanisms implies the nucleation and growth of iPP in the remaining melted iPP bulk that gets retarded by the dispersed POSS network structures. Therefore, we suggest that the first peak of multi-crystallization mechanisms is "*crystallization with the nucleation event assisted by the POSS domains*" on the other hand, that of second peak is "*nucleation and growth of iPP in the remaining bulk melted iPP region*". Thus, at lower crystallization temperatures, the multi-crystallization mechanisms become a single peak during crystallization as shown in Fig. 2. It indicates that the shorter time needed to reach the second peak of multi-crystallization mechanisms due to faster nucleation rate of the neat iPP in bulk region was observed; therefore, second peak of multi-crystallization mechanisms shifts to shorter time scale and combines with the nucleation event assisted by the POSS domains together to form a single exothermic peak during isothermal crystallization.

The effects of POSS content on the relative crystallinity versus crystallization time for iPP/POSS composites are shown in Fig. 3. It shows that the relative crystallinity curve of the pure iPP and POSS-1.0 is sigmoidal, whereas that of POSS-2.0 and POSS-3.0 gives a deviate-sigmoidal curve. The characterization of deviate-sigmoidal curves implies combining a "*nucleating agent inducing nucleation of iPP event assisted by the POSS domains*" during the initial stage process with a "*nucleation and growth of iPP in the remaining bulk melted iPP region*" process during the later stages of isothermal crystallization.

Fig. 4 shows the effects of POSS content on the plot of $\log\{-\ln[1-X(t)]\}$ versus $\log t$. The overall crystallization rate is may be due to the change either in the crystal growth rate or in the nucleation rate. The kinetic parameters of Avrami equation, such as n and k can be determined with fit of the initial stage data [21]. From the results of Fig. 4 and Table 2, the number of Avrami exponents, n value, of isothermal crystallization of iPP/POSS composites increases with

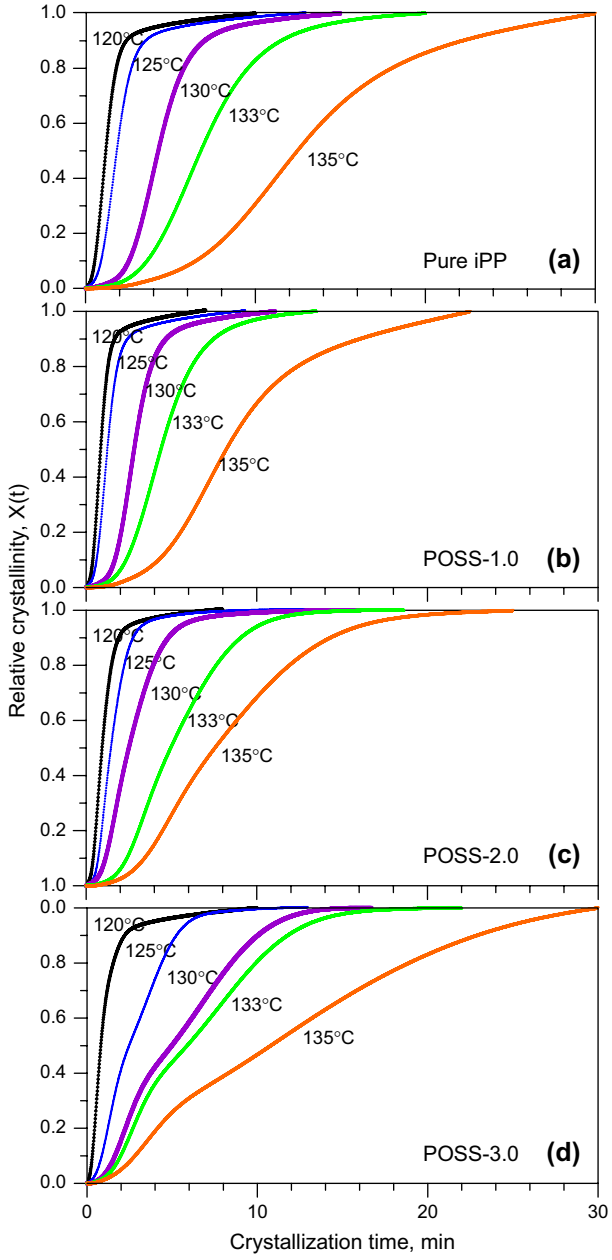

Fig. 3. Effect of POSS contents and crystallization temperature on the relative crystallinity of iPP/POSS composites: (a) pure iPP, (b) POSS-1.0, (c) POSS-2.0, and (d) POSS-3.0.

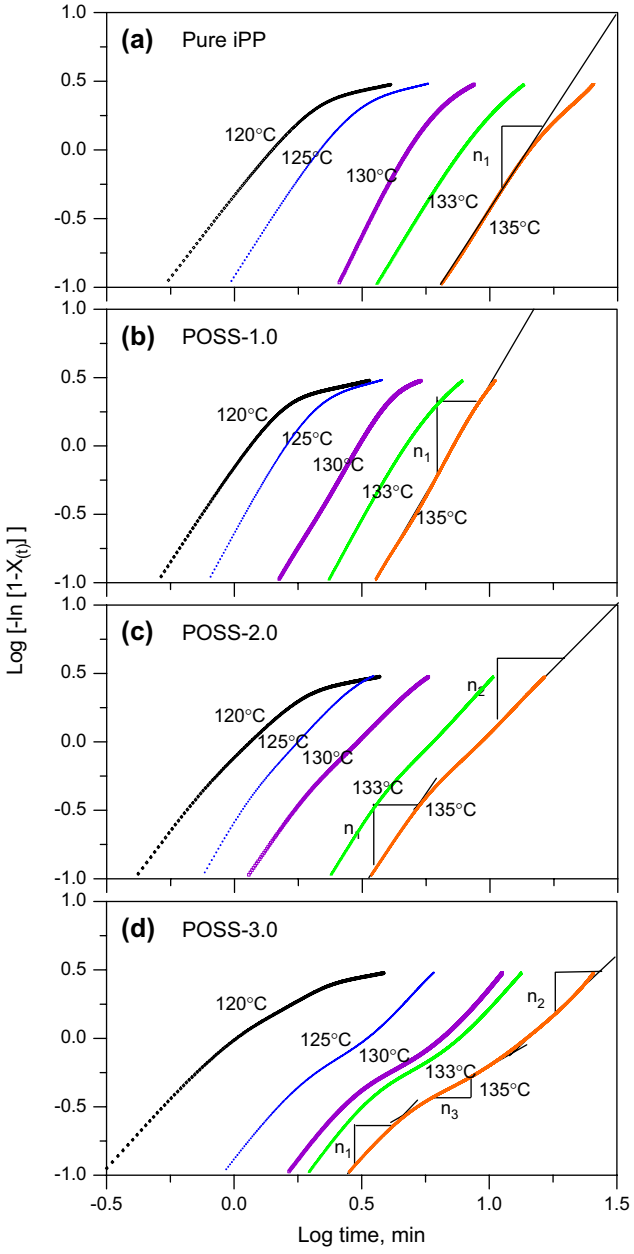

Fig. 4. Effect of POSS contents and crystallization temperature on the Avrami plots of iPP/POSS composites: (a) pure iPP, (b) POSS-1.0, (c) POSS-2.0, and (d) POSS-3.0.

increasing POSS content. For the pure iPP and POSS-1.0, it clearly indicates that the slope of the plots remains unchanged until a higher degree of conversion was reached and shows a single/major exponent, n_1. While the slope of the plots for POSS-2.0 and POSS-3.0 tends to drop at medium degree of conversion as T_c and POSS contents were increased and shows the multi-exponents; n_1, n_2, and n_3 (transfer region) during crystallization. In this work, the Avrami exponents, n_1 and n_2 values, of isothermally crystallized iPP/POSS composites are non-integral and in the range between 2 and 4. An increase in the Avrami exponent is usually attributed in the literature to changing from instantaneous to sporadic nucleation or increasing the dimension of crystal growth [21]. The non-integral n value may be considered due to the crystal branching and/or two-stage crystal growth and/or mixed growth and nucleation mechanism [22,25]. Generally, the n value of iPP is about 3–4 [22,23], some authors have reported the n values in the range of 2 [22] to 4 [24] for iPP blends. The n_1 value for pure iPP and POSS-1.0, in this work, is ca. 2.9 ± 0.3, and that for POSS-2.0 and POSS-3.0, respectively, is ca. 2.5 ± 0.4 over the isothermal crystallization temperature range studied as shown in Table 2. However, for the pure iPP and POSS-1.0, the n_1 value close to 3 indicates a thermal nucleation process followed by a three-dimensional crystal growth. On the other hand, the n_1 value for POSS-2.0 and POSS-3.0 close to 2.5 indicates may hint a thermal nucleation process followed by

Table 2
The isothermal crystallization kinetics of iPP/POSS composites

Samples	T_c (°C)	$t_{1/2}$ (min)	n_1	k_1 (°C min^{-1})	n_2	k_2 (°C min^{-1})	n_3	k_3 (°C min^{-1})
Pure iPP	120	1.19	2.39	46.8 E-02	–	–	–	–
	125	1.89	2.88	11.7 E-02	–	–	–	–
	127	2.74	2.92	6.02 E-02	–	–	–	–
	130	4.28	3.65	3.09 E-03	–	–	–	–
	133	6.77	3.04	2.09 E-03	–	–	–	–
	135	12.47	2.88	4.79 E-04	–	–	–	–
POSS-1.0	120	1.09	2.38	70.8 E-02	–	–	–	–
	125	1.57	2.80	22.4 E-02	–	–	–	–
	127	2.07	3.06	4.27 E-03	–	–	–	–
	130	2.81	3.27	8.13 E-03	–	–	–	–
	133	4.36	3.16	5.75 E-03	–	–	–	–
	135	8.12	3.04	1.04 E-03	–	–	–	–
POSS-2.0	120	0.95	2.40	89.1 E-02	1.51	85.1 E-02	–	–
	125	1.51	3.07	25.1 E-02	2.05	30.2 E-02	–	–
	127	1.86	2.78	11.0 E-02	1.94	19.1 E-02	–	–
	130	2.53	2.69	7.59 E-02	1.86	12.6 E-02	–	–
	133	4.94	3.02	7.76 E-03	2.13	2.34 E-02	–	–
	135	7.47	2.81	3.31 E-03	1.79	1.86 E-02	–	–
POSS-3.0	120	0.81	2.00	112 E-02	1.72	27.3 E-02	1.09	102 E-02
	125	2.53	2.31	12.9 E-02	1.85	10.5 E-02	1.27	20.9 E-02
	127	3.86	2.56	7.41 E-02	1.92	4.27 E-02	1.12	17.4 E-02
	130	4.98	2.41	3.24 E-02	2.28	1.20 E-02	1.06	12.6 E-02
	133	5.97	2.42	1.95 E-02	2.10	1.29 E-02	1.07	1.02 E-02
	135	11.23	2.07	1.23 E-02	1.99	4.57 E-03	1.10	5.01 E-02

mixing two-dimensional and three-dimensional crystal growths, respectively, as discussed in Figs. 8 and 9. However, the slope of the plots for POSS-2.0 and POSS-3.0 drops at medium degree of conversion and shows the multi-exponents with increasing T_c and POSS contents. These facts mean that the multi-exponents take place in POSS-2.0 and POSS-3.0 due to combination of different crystallization mechanisms together; that is the "*nucleating agent inducing nucleation of iPP event assisted by the POSS domains*" and "*nucleation and growth of iPP in the remaining bulk melted iPP region retarded by dispersed POSS molecules*" mechanisms as discussed. Therefore, change in the crystallization mechanism at lower conversion indicates that POSS molecules increase remarkably in nuclei amount and retardation in the growth rate of iPP spherulites by reducing the mobility of iPP chain with dispersed POSS molecule was observed. Thus, the value of Avrami exponents for second peak of multi-crystallization mechanisms, n_2, is about 2.0 ± 0.2, and that for transfer region, n_3, drops to about 1.2. The lower n values were attributed to two- or one-dimensional crystal trapped within the spherulites during crystallization. These isothermal crystallization kinetic parameters are summarized in Table 2.

The half-time of crystallization, $t_{1/2}$, represents the time to reach the maximum rate of heat flow and corresponds to the change over to a slower kinetic process due to impingement of adjacent spherulites [26]. In this work, the result indicates that the $t_{1/2}$ decreases with increasing POSS content and ΔT at lower than 2 wt% of POSS, therefore, this fact clearly proves that the POSS molecules play the role as an essential nucleating agent for iPP and promotes nucleation rate of iPP chains at small loading of POSS during isothermal crystallization. From the isothermal crystallization, the growth rate of crystallization, G, defined as $G = 1/t_{1/2}$, is obtained from endotherm morphology of DSC analysis. The growth rate of crystallization can be expressed as follows according to the Hoffman and Lauritzen theory [27]:

$$G = G_0 \exp\left[-\frac{U^*}{R(T_c - T_\infty)}\right] \exp\left[-\frac{K_g}{T_c \Delta T f}\right] \tag{5}$$

where G_0 is a pre-exponential term, R is the universal gas constant, U^* is the energy of the transport of the chains in the melt, T_c is the crystallization temperature, T_∞ is the temperature where all the motions associated with the viscous flow stop, defined as $(T_g - C)$ where C is a constant; ΔT is the supercooling temperature, defined as $\Delta T = T_m^o - T_c$; f is corrective factor that takes into account the variation of the equilibrium melting enthalpy, ΔH_m^o, with temperature, defined as $(2T_c/(T_c + T_m^o))$; K_g is a term connected with the energy required for the formation of nuclei of critical size, defined as $nb\sigma\sigma_e T_m^o/\Delta H_m^o k$; and n is a variable that considers the crystallization regime and assumes the value 4 for the regimes I and III, and the value 2 for the regime II [28].

The spherulite radial growth rate, G, as a function of crystallization temperature, T_c and POSS content is reported in Fig. 5 for the pure iPP and iPP/POSS composites. For all the samples, radial growth rate decreases with the T_c. This result is in agreement with the kinetic theory of crystallization that expects for crystallizations close to T_m, a decrease of G reducing the supercooling temperature, ΔT. As the POSS

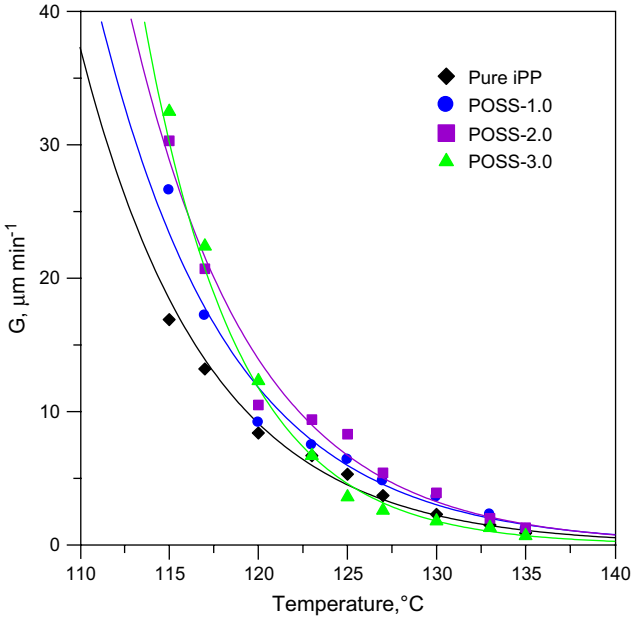

Fig. 5. Effect of POSS contents and crystallization temperature on the spherulite radial growth rate, G, during isothermal crystallization.

molecules are added, the G of iPP matrix decreases, at temperature below 123 °C, on the other hand, at temperature above 123 °C, the G increases and then decreases with the POSS content. It indicates that the dispersed POSS molecules can both influence the terms of transportability of the iPP chain in melt region and formation of the critical nuclei during crystallization. Therefore, the depression of G at higher crystallization temperatures confirms that the transportability of iPP chains in the melt is the factor that dominates the crystallization process of the iPP/POSS composites. In this case of iPP/POSS composites, the presence of the POSS molecules can both influence the terms of transport of the iPP chain in molten region and formation of the critical nucleus. In fact, during the crystallization the major dispersed POSS molecules form nanocrystals first that appears as an effective nucleating agent and then these POSS nanocrystals aggregate together to form thread or network nanocrystal structures in molten state of iPP that can greatly disturb the nucleation and growth rates of iPP by the POSS structures due to change in the energetic barrier of formation in the critical nucleus and transportability of iPP in the melted state. On the other hand, the minor dispersed POSS molecules, which is slightly miscible with iPP, in molten iPP region must reduce the transportability of the iPP chain. Therefore, the energy constituting a new energetic barrier that can control the nucleation and growth of iPP, during isothermal crystallization, is very complex in this study.

3.3. Thermal behavior of isothermally crystallized iPP/POSS composites

Fig. 6(a)–(d) presents the melting behavior of isothermally crystallized iPP/POSS composites at different POSS contents and crystallization temperatures. However, the feature of melting profile of iPP/POSS composites appears as two melting endotherms at POSS content lower than 2 wt% and T_c lower than 130 °C, while shows a single melting endotherm at POSS content higher than 3 wt% and T_c higher than 130 °C. It is clearly indicated that, by increasing the POSS content and T_c, the heat of fusion of the lower-temperature endotherm, ΔH_f^L, decreases, while the heat of fusion of the higher-temperature endotherm, ΔH_f^H, increases, respectively. The existence of double melting endotherm peaks in the DSC profiles may result from the following reasons: (1) the presence of two different crystal structures or the presence of two different thicknesses of crystal lamellae with the same type of crystal structure formed at the isothermal crystallization conditions [29], and (2) the simultaneous melting–reorganization–remelting of the lamellae originally formed during the crystallization process [30]. The result of melting profile indicates that may be more stable or perfect crystal of iPP was observed with increasing POSS content and T_c. The heat of fusion and morphology of the two endotherms were found to be dependent on the POSS content and T_c, and so the crystallinity and morphology of iPP/POSS composites after isothermal crystallization are also affected by the POSS content and T_c.

The melting profile shows that the area of the ΔH_f^L decreases with increasing T_c which is the indication of reducing recrystallization or reorganization of the crystals originally formed during crystallization. Moreover, the area of the ΔH_f^H increases with increasing T_c, because a higher degree of perfection or higher stable crystal was achieved in the crystals initially obtained as discussed by Corradini et al. [31,32]. At temperature below 127 °C, the ΔH_f^L and melting temperature of lower-endotherm, T_m^L, remain almost constant, and then the ΔH_f^L disappears at T_c higher than 130 °C. This result implies that the previous thermal history or degree of perfection achieved for iPP/POSS composites may be the same at T_c below 127 °C. On the other hand, both of the ΔH_f^H and melting temperature of higher-endotherm, T_m^H, increase with increasing T_c. On the other hand, increasing the POSS content led to retardation of the mobility of iPP chains in the melted state and reduces the iPP chain to allow the recrystallization at higher temperatures to takes place, and so a more stable crystal was formed at higher POSS. Therefore, occurrence of the double melting peaks at lower POSS content may be mainly caused by simultaneous melting–reorganization–remelting of the lamellae during heating trace. While, at POSS content above 3 wt%, the melting profile shows a single melting endotherm may be due to more stable crystal of iPP that retarded the melting–reorganization–remelting by the network structure of POSS nanocrystals was observed. However, the isothermal crystallization temperature and blending content caused the distributions of the double melting endotherms of iPP/aPP blends which have been reported recently [33].

For all isothermal crystallization temperatures of iPP/POSS composites investigated, the observed T_m^H linearly increases with the T_c. Thus to determine the equilibrium melting temperature, T_m^o, recorded using the Hoffmann–Weeks equation [34], a plot of T_c versus T_m with a line is drawn where $T_c = T_m$. The

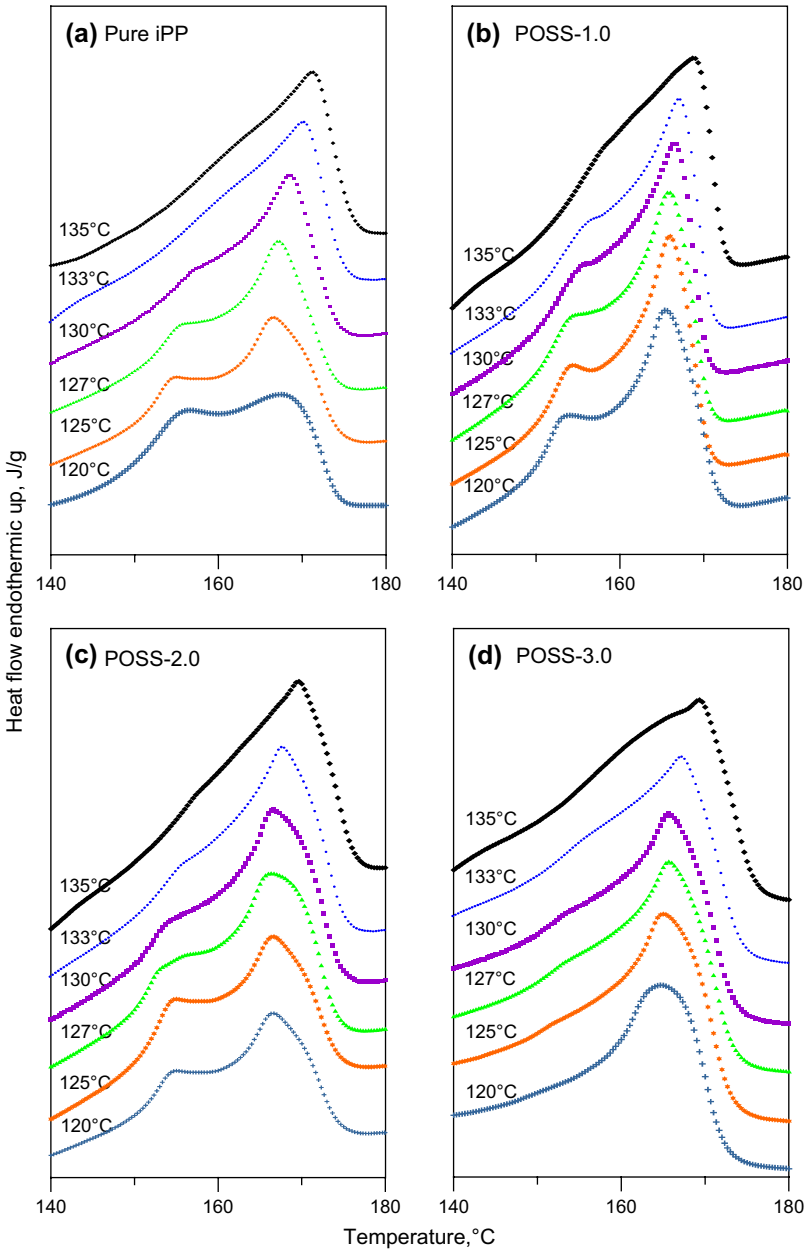

Fig. 6. Melting endotherm of iPP/POSS composites after isothermal crystallization for 120 min at different isothermal temperatures: (a) pure iPP, (b) POSS-1.0, (c) POSS-2.0, and (d) POSS-3.0.

experimental data can be extrapolated to the intersection of the line; the intersection is the T_m^o as following relation:

$$T_m^o - T_m = \phi'\left(T_m^o - T_c\right) \tag{6}$$

where ϕ' represents a stability parameter that depends on crystal size and perfection. Fig. 6 indicates the melting temperatures registered at the T_m^H versus different T_c for the isothermally crystallized iPP/POSS composites. A straight line was extrapolated from the experimental T_m^H values of iPP/POSS composites with different T_c, and the calculated T_m^o for all iPP/POSS composites was observed. The effects of POSS content on the T_m^o of iPP/POSS composites are shown in Fig. 7. The result illustrates that the T_m^o decreases slightly as POSS was added. The T_m^o of pure iPP is ca. 187.8 °C, while the values of T_m^o, for POSS-1.0, POSS-2.0, and POSS-3.0, respectively, are ca. 185.9, 186.6, and 186.6 °C, respectively. This result implies that the POSS nanocrystals act as an effective nucleating agent for iPP and promote the crystallization rate of iPP; and so the T_m^o decreases slightly due to more imperfect iPP crystal, at POSS content above than 2 wt%, as discussed above.

3.4. Development of spherulitic morphologies of iPP/POSS composites

The morphology development and size of spherulites for iPP/POSS composites at very small loading of POSS were

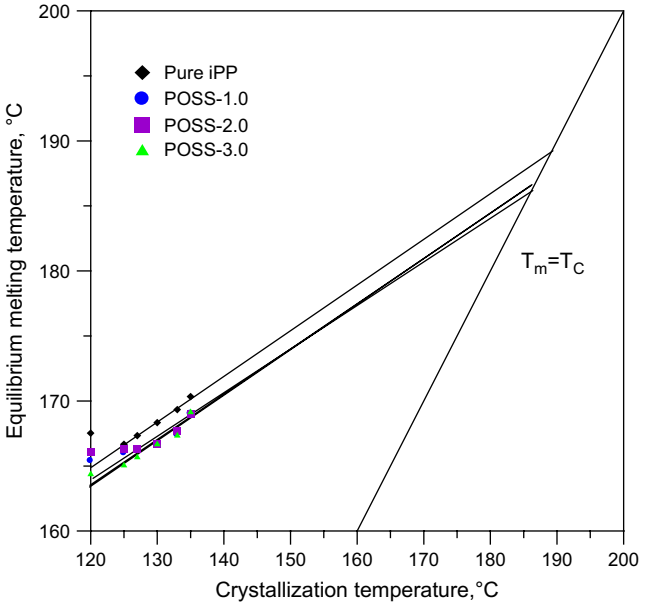

Fig. 7. Plot of the observed equilibrium melting temperature, T_m^o, by linearly increases the melting temperature of the higher-endothermic, T_m^H, for iPP/POSS composites with the crystallization temperature, T_c, recorded using the linear Hoffman–Weeks extrapolation.

also investigated with polarized optical microscopy at 130 °C as shown in Fig. 8. Fig. 8(a) and (b) displays the morphology development of spherulites of pure iPP at different crystallization times. It indicates that the pure iPP may hint a sporadic nucleation process followed by a three-dimensional crystal growth which is in agreement with the result of DSC. Comparably, the morphology development of spherulites for POSS-1.0, POSS-3.0, and POSS-5.0 shows the instantaneous nucleation process followed by a three- and two-dimensional crystal growths as shown in Fig. 8(c)−(h), respectively, during crystallization. It is interesting to note that the nucleation process for POSS-3.0 and POSS-5.0 shows heterogeneous nucleation process with thread- or network-like structure, which depends on the POSS content, in the initial step of crystallization. It indicates that the dispersed POSS nanocrystals aggregate together forming the thread- or network-like structure because the interaction force between POSS nanocrystals is larger than that between POSS nanocrystals and iPP chain as reported recently [8]. At the analyzed crystallization temperatures, the morphological results for all the iPP/POSS composites, the decrease of G with POSS at T_c above 120 °C is surely to be ascribed to the nucleation and transport rates of iPP in the remaining bulk melted iPP region retarded by dispersed POSS molecules as discussed. Therefore, the presence of the dispersed POSS molecules produces a change in both the energies relative to the transportability and to the formation of the nuclei of critical dimension of iPP. Fig. 9 displays a thread- or shish−kebab-like morphology of POSS-2.0 at 130 °C with polarized optical microscopy. From the result of Fig. 9, it is clearly showed that there are two types of spherulites in the POSS-2.0 at 130 °C. The first type is the spherulites nucleated from the surface of thread-like POSS structure. The nucleation of these spherulites is fast, and although the subsequent growth may be slower, the corresponding overall crystallization rate (containing contribution from both nucleation and growth) is still faster than that of neat iPP. The second type is the spherulites nucleated in the remaining bulk melted iPP region. The nucleation of these spherulites was not assisted by POSS and their growth may be retarded by the slight miscibility between iPP and POSS. Therefore, the overall crystallization associated with the formation of these spherulites was slower and hence contributed to the second exotherm. On the other hand, the spherulitic morphology and growth process clearly indicate that the iPP/POSS composites may hint a thread-like nucleation assisted by the POSS nanocrystals and followed by a three- and two-dimensional crystals' growth of iPP was also shown in Fig. 9.

3.5. Development of microstructure of iPP/POSS composites

Fig. 10 shows the WAXD intensity profiles of iPP/POSS composites after isothermal crystallization at 130 °C. The X-ray diffractograms of iPP/POSS composites show nearly the α-form diffractograms of iPP after isothermal crystallization. For the isothermally crystallized iPP, the characteristic peaks of the α-form crystal of iPP can be found at 2θ angles of 14.08° (110), 16.95° (040), 18.5° (130), 21.2° (111), and 21.85° (−131 and 041) as diffractogram marked of pure iPP in Fig. 12 [35−37]. As seen, the X-ray diffraction profiles show that the crystallinity of POSS in the iPP/POSS nanocomposites is very high, even at very small loading of POSS (POSS-1) can also see clearly the (011) reflection planes of POSS crystal at $2\theta = 11.0°$. The intensity of (011) reflection planes of POSS crystals increases, but the breadth of (011) reflection plane does not change remarkably with increasing POSS contents. It implies that the amount of POSS nanocrystals increases, but the crystal size of POSS nanocrystals does not change remarkably with increasing POSS contents. These results indicate that the POSS crystals were formed in nanocrystals in the iPP/POSS nanocomposites. The majority of POSS molecules in iPP/POSS composites was formed by about 35 nm of rhombic nanocrystals as reported recently [8].

Fig. 11 shows the effects of the POSS content on the isothermal crystallization mechanism of iPP/POSS composites at 130 °C. By increasing the POSS content, the crystallization mechanism morphology from a single exothermic peak transfers to multi-exothermic peaks as discussed above. In this study, we suggest that the single exothermic peak of pure iPP attributes to the "*crystallization with the homogeneous nucleation*", while that of POSS-1.0 to the "*nucleating agent inducing nucleation of iPP event assisted by the POSS domains*". On the other hand, at higher POSS content, the first peak of multi-crystallization mechanisms attributes to the "*nucleating agent inducing nucleation of iPP event assisted by the POSS domains*", while, the second peak of multi-crystallization mechanisms attributes to the "*nucleation and growth of iPP in the remaining bulk melted iPP region*" as discussed above.

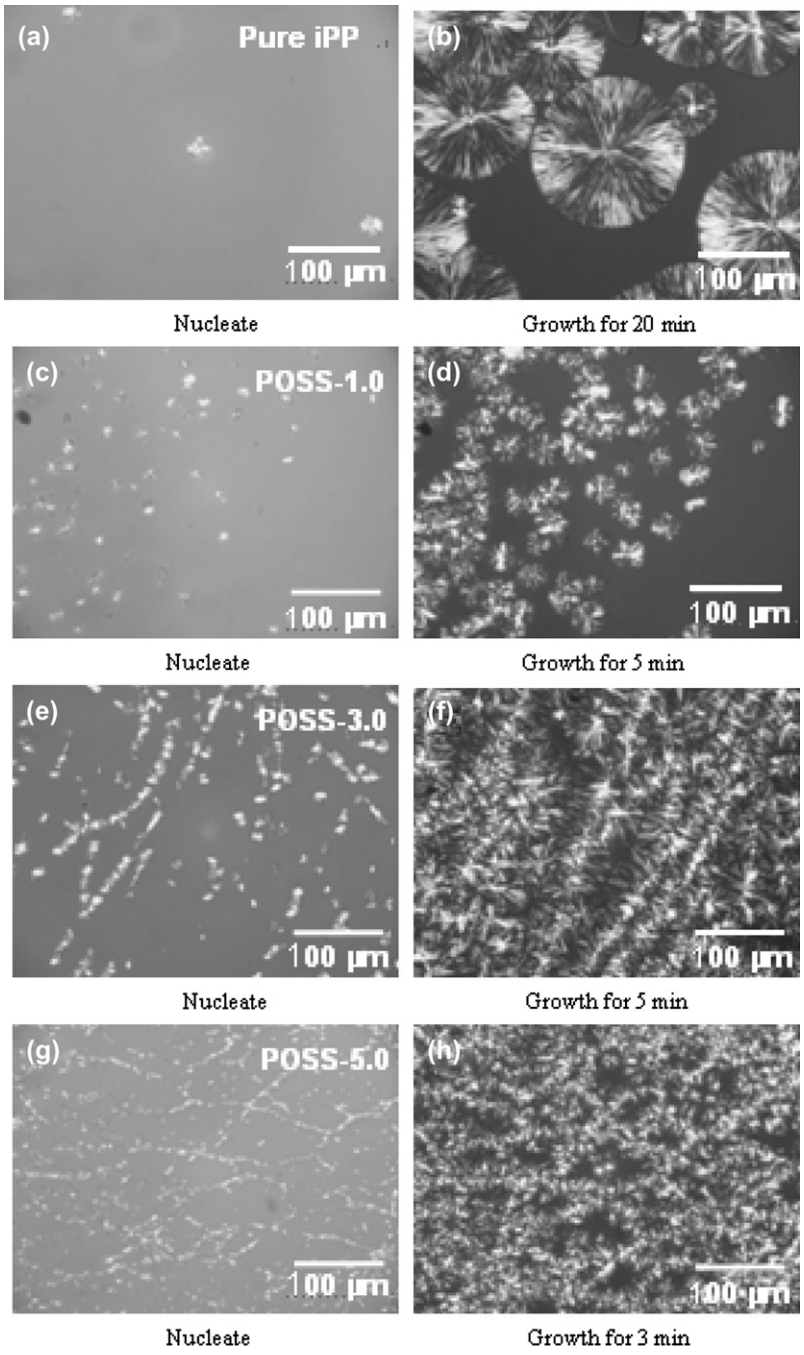

Fig. 8. Spherulitic morphologies of crystallization process of iPP/POSS composites with various POSS content at 130 °C, magnification 400×: (a) nucleate, (b) growth for 20 min of pure iPP; (c) nucleate, (d) growth for 5 min of POSS-1.0; (e) nucleate, (f) growth for 5 min of POSS-3.0; (g) nucleate, and (h) growth for 3 min of POSS-5.0.

Therefore, the effects of the POSS content on the overall areas in the multi-crystallization peaks for isothermal crystallization mechanisms of iPP/POSS composites were determined. The effect of POSS molecules on the fraction contents of "*crystallization with the nucleation event assisted by the POSS domains*" and "*growth of iPP in the remaining bulk melted iPP region retarded by dispersed POSS molecules*" is then calculated on the basis of the relative area of multi-exothermic peaks as below equations:

$$F_{\mathrm{nuc}} = A_{\mathrm{firs}} / \left[A_{\mathrm{firs}} + A_{\mathrm{secon}}\right] \tag{7}$$

$$F_{\mathrm{bulk}} = A_{\mathrm{secon}} / \left[A_{\mathrm{firs}} + A_{\mathrm{secon}}\right] \tag{8}$$

where A_{firs} and A_{secon} are areas of first and secondary peaks for multi-crystallization mechanisms, respectively, and F_{nuc} and F_{bulk} are fraction contents of crystallization mechanism for "*crystallization with the nucleation event assisted by the*

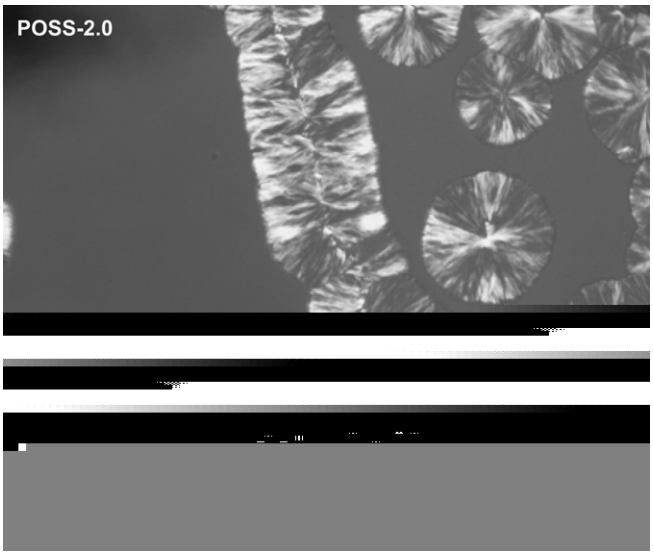

Fig. 9. Growth process of thread- or shish–kebab-like spherulitic morphology for POSS-2.0 at 130 °C, magnification 400×.

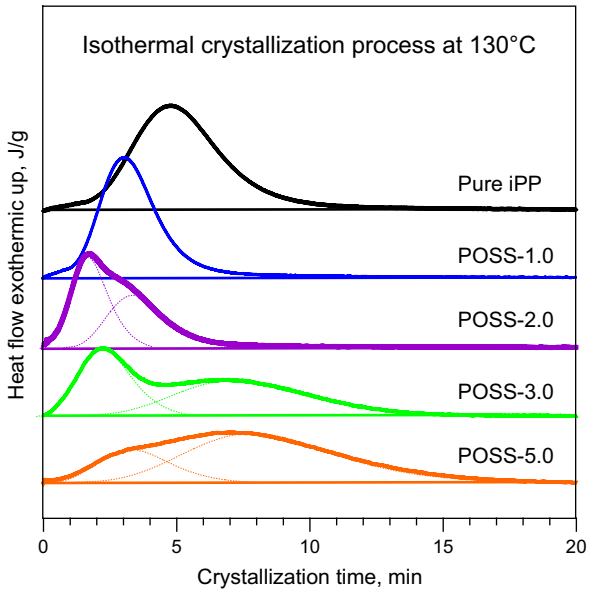

Fig. 11. Influence of the POSS contents on the isothermal crystallization mechanisms of iPP/POSS composites at 130 °C.

POSS domains" and "*growth of iPP in the remaining bulk melted iPP region retarded by dispersed POSS molecules*", respectively. Fig. 12 shows the dependence of the POSS contents on the fraction content of multi-crystallization mechanisms of iPP/POSS composites. As POSS contents increased, the fraction content of crystallization with the nucleation event assisted by the POSS domains decreases remarkably from about 100% to 21.2%, while that of growth of iPP in the remaining bulk melted iPP region is retarded by dispersed POSS molecules increasing from 0% to 78.8% during crystallization at 130 °C. This result indicates that the crystallization with the nucleation event assisted by the POSS domains' mechanism plays a dominant role for multi-crystallization mechanisms at POSS content lower than 2.5 wt%, while the growth of iPP in the remaining bulk melted iPP region retarded by dispersed POSS molecules' mechanism presents a major role for multi-crystallization mechanisms at POSS content higher than 2.5 wt%. The growth of iPP in the remaining bulk melted iPP region is retarded by dispersed POSS molecules increases remarkably at POSS contents above 2.5 wt% due to the dispersed POSS molecules aggregate remarkably and forming

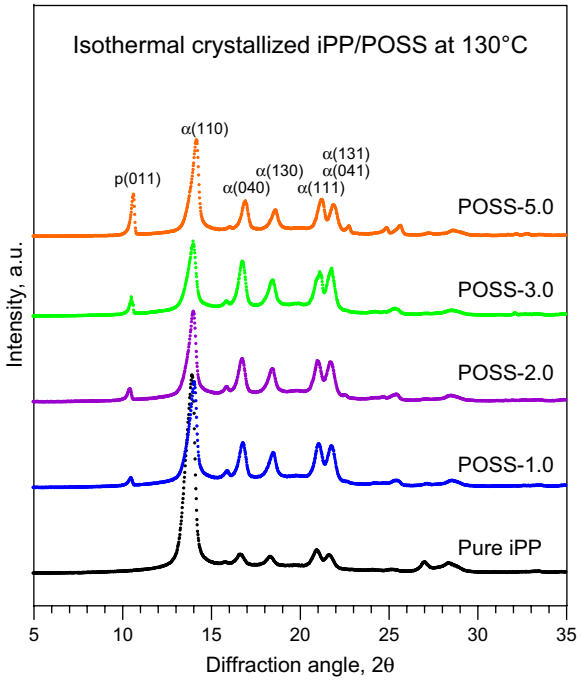

Fig. 10. WAXD intensity patterns of isothermally crystallized iPP/POSS composites at 130 °C.

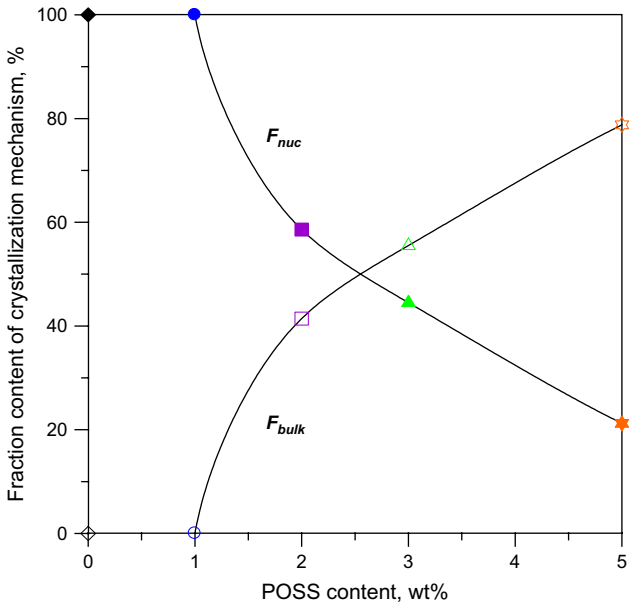

Fig. 12. Influence of the POSS contents on the fraction content of multi-crystallization mechanisms of iPP/POSS composites: (○) nucleating agent inducing nucleation of iPP event assisted by the POSS domains, F_{nuc}, and (●) nucleation and growth of iPP in the remaining bulk melted iPP region, F_{bulk}.

network-like structure to retard the growth rate of iPP in the iPP/POSS composites as discussed in Fig. 6. Therefore, these results demonstrate that the miscibility between POSS molecules and iPP matrix is poor because the interaction forces between POSS molecules (dipole–dipole interaction between oxygen atoms on the POSS cage) remarkably larger than that between POSS molecules and iPP matrix (dispersion force between methyl groups on the POSS cage and polypropylene).

4. Conclusions

In this study, the POSS molecules in iPP/POSS composites aggregated together to form the thread- or network-like nanocrystal structures that promote or retard the isothermal and nonisothermal crystallization behaviors of iPP, at very small loading of POSS, were demonstrated. However, the iPP/POSS composites showed the single and double melting endotherms, respectively, depending on POSS molecules during heating trace. The existence of double melting endotherms may be due to simultaneous melting–reorganization–remelting of the lamellae, while, the single melting endotherm may be due to the network structure of POSS nanocrystals that retarded the melting–reorganization–remelting during heating trace. On the other hand, at cooling trace, the time needed to reach the exothermic maximum of crystalline order, t_{em}, both the isothermal and nonisothermal crystallizations for iPP/POSS composites rapider than that of pure iPP. Moreover, the Avrami exponents and spherulitic morphologies of pure iPP and POSS-1.0 exhibited a sporadic and heterogeneous nucleation, respectively, followed by a three-dimensional crystal growth of iPP. Whereas that of POSS-3.0 and POSS-5.0 showed a heterogeneous nucleation process followed by a combination of two- and three-dimensional crystals growths, respectively, depending on POSS content. These results clearly indicated that the major dispersed POSS molecules in iPP/POSS composites became nanocrystal first that appears as an effective nucleating agent and then these POSS nanocrystals aggregate together to form thread or network nanocrystal structures in molten state of iPP that can greatly disturb the nucleation and growth rates of iPP by the POSS structures due to change in the energetic barrier of formation in the critical nucleus and transportability of iPP in melted state. On the other hand, the minor dispersed POSS molecules in the melted iPP region must reduce the transportability of the iPP chain.

Therefore, in the isothermal crystallization process, both the pure iPP and POSS-1.0 showed a single exothermic peak with different T_c, comparatively, the POSS-2.0 to POSS-5.0 exhibited the multi-exothermic peaks at higher T_c. These results indicate that the crystallization mechanism of pure iPP proceeds mainly via homogeneous nucleation, while that of POSS-1.0 proceeds by heterogeneous or nucleating agent inducing crystallization mechanism, respectively. On the other hand, the crystallization mechanisms of POSS-2.0 to POSS-5.0 proceed by combining the "*crystallization with the nucleation event assisted by the POSS domains*" and "*nucleation and growth of iPP in the remaining bulk melted iPP region retarded by dispersed POSS molecules*" mechanisms that depended on the POSS content and T_c. Thus, in this study, the crystallization with the nucleation event assisted by the POSS domains' mechanism played a dominant role for the multi-crystallization mechanisms at POSS content lower than 2.5 wt%, while the nucleation and growth of iPP in the remaining bulk melted iPP region retarded by dispersed POSS molecules' mechanism presented a major role at POSS content higher than 2.5 wt%. Therefore, these results indicated that at higher POSS contents showed to be more favorable aggregated to form the thread- or network-like structures of major POSS nanocrystals and retarded the mobility or diffusion ability of iPP chain by the minor dispersed POSS molecules during crystallization. From above result, therefore, we postulated that the strong interaction between POSS molecules (dipole–dipole interaction between oxygen atoms on the POSS cage) and weak interaction between POSS and iPP matrix (dispersion force between methyl groups on the POSS cage and polypropylene) dominated the isothermal and nonisothermal crystallization behaviors of iPP/POSS composites at quite low loading of POSS due to the major POSS nanocrystals' morphologies appeared as an effective nucleating agent and promoted the nucleation rate of iPP, whereas the minor dispersed POSS molecules that is slightly miscible between iPP retarded the nucleation and growth rates of iPP in the remaining bulk region during crystallization.

Acknowledgements

The authors thank Dr. H.L. Chen for the useful discussions and the research facility of WAXD provided by the Nano-Technology Research and Development Center, Kun Shan University. This work was supported by the National Science Council of the Republic of China through grant NSC 93-2216-E-168-004.

References

[1] Tang J, Wang Y, Liu H, Belfiore LA. Polymer 2004;45:2081.
[2] Marco C, Ellis G, Gomez MA. J Appl Polym Sci 2002;84:2440.
[3] Chan CM, Wu JS, Li JX. Polymer 2002;43:2981.
[4] Fu BX, Yang L, Somani RH, Zong SX, Hsiao BS, Phillips S, et al. J Polym Sci Part B Polym Phys 2001;39:2727.
[5] Fu BX, Gelfer MY, Hsiao BS, Phillips S, Viers B, Blanski R, et al. Polymer 2003;44:1499.
[6] Fina A, Tabuani D, Frache A, Camino G. Polymer 2005;46:7855.
[7] Joshi M, Butola BS. Polymer 2004;45:4953.
[8] Chen JH, Chiou YD. J Polym Sci Part B Polym Phys 2006;44:2122.
[9] Lichtenhan JD. Comments Inorg Chem 1995;17:115.
[10] Haddad TS, Lichtenhan JD. Macromolecules 1996;29:7302.
[11] Mantz RA, Jones PF, Chaffee KP, Lichtenhan JD, Gilman JW, Ismail IBM, et al. J Chem Mater 1996;8:1250.
[12] Mater PT, Jeon HG, Romo-Uribe A, Haddad TS, Lichtenhan JD. Macromolecules 1999;32:1194.
[13] Fu BX, Hsiao BS, Pagola S, Stephens P, White H, Rafailovich M, et al. Polymer 2000;42:599.
[14] Bharadwaj RK, Berry RJ, Farmer BL. Polymer 2000;41:7209.
[15] Wu HD, Chu PP, Ma CCM, Chang FC. Macromolecules 1999;32:3097.
[16] Xu H, Kuo SW, Lee JS, Chang FC. Macromolecules 2002;35:8788.
[17] Zheng L, Farris RJ, Coughlin EB. Macromolecules 2001;34:8034.
[18] Zheng L, Kasi RM, Farris RJ, Coughlin EB. J Polym Sci Part A Polym Chem 2002;40:885.

[19] Avrami M. J Chem Phys 1940;8:212.
[20] Avrami M. J Chem Phys 1941;9:177.
[21] Wunderlich B. Macromolecular physics, vol. 1. New York: Academic Press; 1976. p. 21.
[22] Wunderlich B. Macromolecular physics, vol. 2. New York: Academic Press; 1976. p. 115.
[23] Godovskii YK. Polym Sci USSR 1969;11:2423.
[24] Carfagna C, Derosa C, Guerra G, Petraccone V. Polymer 1984;25:1462.
[25] Jonsson H, Wallgren E, Hult A, Gedde UW. Macromolecules 1990;23: 1041.
[26] Bodor G. Structural investigation of polymers. Chichester: Ellis Horwood; 1991.
[27] Hoffman JD, Davis GT, Lauritzen JI. In: Hannay NB, editor. Treatise on solid state chemistry, vol. 3. New York: Plenum Press; 1976. p. 7.
[28] Hoffman JD. Polymer 1982;24:3.
[29] Cebe P, Hong SD. Polymer 1986;27:1183.
[30] Holdsworth PJ, Turner-Jones A. Polymer 1971;12:195.
[31] Corradini P, Napolitano R, Oliva L, Petraccone V, Pirozzi B. Makromol Chem Rapid Commun 1982;3:753.
[32] Guerra G, Petraccone V, Corradini P, Rosa CD, Napolitano R, Pirozzi B, et al. J Polym Sci Polym Phys Ed 1984;22:1029.
[33] Chen JH, Tsai FC, Nien YH, Yeh PH. Polymer 2005;46:5680.
[34] Hoffman JD, Weeks JJ. J Chem Phys 1965;42:4301.
[35] Brückner S, Meille SV, Petraccone V, Pirozzi B. Prog Polym Sci 1991; 16:361.
[36] Phillips RA, Wolkowicz MD. In: Moore EP, editor. Polypropylene handbook. Munich: Hanser; 1996. p. 113.
[37] Mezghani K, Phillips PJ. Polymer 1998;39:3735.